Study for the Elucidation of the Sedimentation Structure Using the Numerical Analysis

Yusaku ISOBE(1), Tomoaki HACHIMURA(2), Hiroyuki OHNO(3), Kenji MATSUMOTO(2), Tetsuya MIYAHARA(2), and Shuichi NAGAOKA (2)

(1) Geoscience Research Laboratory, Co., Ltd., Japan
E-mail: isobe@geolab.jp
(2) Japan Environmental Sanitation Center, Japan, (3) Kankyo Chishitsu, Co., Ltd., Japan

Abstract

Sedimentation in the liquid (the water or the seas) had been thought based on the Stokes' theorem, but the study of authors presented that it did not follow the Stokes' theorem when a sedimentation particle has the large Reynolds number. Tsunami sediment and slump deposit (landslide) are considered as the environment causing the large Reynolds number, and understanding these sedimentation forms will leads to the valuable knowledge for future disaster. Therefore, the authors tried to express the sedimentation phenomenon in the liquid by the numerical analysis technique. It is confirmed that the numerical analysis is able to express the phenomenon that an enormous number of fine particles lose their energy and sank in the liquid at uniform velocity.

Keywords: MPS method, Sedimentation, Numerical analysis

1. Introduction

A turbidite is the geologic deposit of a turbidity current, which is a type of sediment gravity flow responsible for distributing vast amounts of clastic sediment into the deep ocean. The origin of the turbidity current is regarded as the sea landslide and the tsunami with the earthquake, sudden vaporization of the methane hydrate layer, submarine volcano eruption at the bottom of sea. It is related to components such as the methane hydrate to understand sequence of the turbidite formation. In addition, it is very important in disaster prevention and the environment to comprehend how a sea area changes by the landslide. By the cause of such a background, in this study, the numerical analysis has been carried out to express the process of the landslides under the sea water and collision of the sediment with the seafloor. Furthermore, the state that seafloor is stirred up and the sediment lies beneath the sea ground after collision is focused in this research.

2. Numerical Method

2.1 Governing equations

The MPS (Moving Particles Semi-implicit) method (Koshizuka et al., 1996, 1998) is one of the particle methods assuming a material as a particle and expressing the behavior of the material in consideration of influence of the movement among particles by analytical technique. In this approach, a differential equation is discretized using a particle interaction model shown in Fig.1 for a differential operator.

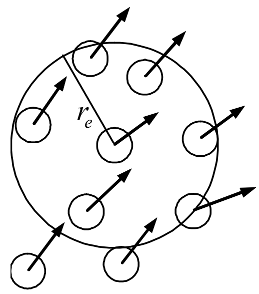

Fig. 1 Concept of the particle interaction model in MPS

A particle interacts with its neighboring particles covered with a weight function $w(r)$, where r is a distance between two particles. The weight function in this study is defined as

$$w(r) = \begin{cases} \dfrac{r_e}{r} - 1 & (0 \le r < r_e) \\ 0 & r_e \le r \end{cases} \tag{1}$$

where r_e is a finite distance. Interactions are restricted to this finite distance.

When a particle i and its neighbors j are located at $\mathbf{r}_i$ and $\mathbf{r}_j$, particle number density is define as

$$n_i = \sum_{j \neq i} w\left(\left|\mathbf{r}_j - \mathbf{r}_i\right|\right) \tag{2}$$

Because an incompressible non-viscous flows is assumed here, the density of the fluid is constant. Therefore, this constant value is assumed n^0 because the particles number density becomes constant.

The gradient operator is modelled using the weight function. A gradient vector is evaluated between two neighboring particles i and j as

$$\left\langle \nabla \phi \right\rangle_{ij} = \frac{\phi_j - \phi_i}{\left|\mathbf{r}_j - \mathbf{r}_i\right|^2}\left(\mathbf{r}_j - \mathbf{r}_i\right) \tag{3}$$

where ϕ is a physical quantity. Here, the angle brackets on the left side of equation indicates a symbol for expressing an interaction model between particles. In MPS, this equation is expressed as below, using the gradient vector at $\mathbf{r}_i$ which is a weighted average of these vectors,

$$\left\langle \nabla \phi \right\rangle_i = \frac{d}{n^0} \sum_{j \neq i} \frac{\phi_j - \phi_i}{\left|\mathbf{r}_j - \mathbf{r}_i\right|^2}\left(\mathbf{r}_j - \mathbf{r}_i\right) w\left(\left|\mathbf{r}_j - \mathbf{r}_i\right|\right) \tag{4}$$

where d is the number of space dimensions. In addition, the particles number density n_i in the location of particle i should be originally adopted, but n^0 is assumed to simplify a calculation.

On the other hand, the divergence theorem is generally expressed in the case of two dimensions.

$$\nabla \cdot \mathbf{u} = \frac{\partial u}{\partial x} + \frac{\partial v}{\partial y} \qquad \mathbf{u} = \left(u, v\right) \tag{5}$$

By this equation, the divergence model used in MPS is defined as

$$\left\langle \nabla \cdot \mathbf{u} \right\rangle_i = \frac{d}{n^0} \sum_{j \neq i} \frac{\mathbf{u}_j - \mathbf{u}_i}{\left|\mathbf{r}_j - \mathbf{r}_i\right|^2} \cdot \left(\mathbf{r}_j - \mathbf{r}_i\right) w\left(\left|\mathbf{r}_j - \mathbf{r}_i\right|\right) \tag{6}$$

Furthermore, the Laplacian model for diffusion in MPS is given as

$$\left\langle \nabla^2 \phi \right\rangle_i = \frac{2d}{\lambda n^0} \sum_{j \neq i} \left(\phi_j - \phi_i\right) w\left(\left|\mathbf{r}_j - \mathbf{r}_i\right|\right) \tag{7}$$

This model is conservative because the quantity lost by a particle i is gained by particles j. Using Equation (7), the Laplacian operator is discretized to simultaneous linear equations with respect to ϕ_i. A parameter λ is introduced so that the variance increase is equal to the analytical solution defined as

$$\lambda = \frac{\sum_{j \neq i} \left|\mathbf{r}_j - \mathbf{r}_i\right|^2 w\left(\left|\mathbf{r}_j - \mathbf{r}_i\right|\right)}{\sum_{j \neq i} w\left(\left|\mathbf{r}_j - \mathbf{r}_i\right|\right)} \tag{8}$$

These models are built and an incompressible non-viscous flows are calculated.

In addition, the different sizes of the weight function are used in this study. The size which is used for the particle number density and the gradient model is r_e=2.1l_0, where l_0 is the distance between two adjacent particles in the initial configuration. The value of 2.1 was selected to avoid the concentration of particles near the free surfaces. On the other hand, the size which is used for the Laplacian model is r_e=4.0l_0 (Koshizuka et al., 1996, 1998). The value of 4.0 was selected by the balance between computation time and accuracy.

Governing equations are expressed by conservation laws of mass and momentum. Kinematic viscous flows are considered in this study.

$$\frac{D\rho}{Dt} = 0 \tag{9}$$

$$\frac{D\mathbf{u}}{Dt} = -\frac{1}{\rho}\nabla P + \nu \nabla^2 \mathbf{u} + \mathbf{g} \tag{10}$$

where, ρ is the density, P is the pressure, **u** is the velocity vector, ν is kinematic viscosity, and g is gravity vector.

The Equation (9) is the law of conservation of mass, and the mass conservation equation is represented by density, while velocity divergence is usually used in the finite difference method. The Equation (10) is called Navier-Stokes equations, and the left side of Equation (10) is the Lagrangian derivative involving advection terms. In MPS, the advection terms are directly incorporated into the calculation by moving particles. Only gravity is considered as the external force. Two-dimensional problems are solved in this study.

Although these equations are expressed as single phase flow, they are extended to multi-phase flow combined with surface tension and rigid body model and multi-phase flow is applied in this paper.

2.2 Stability of the numerical computation

Numerical computation is unstable by explicit calculation of convective term or diffusion term in the semi-implicit difference method. The convective term is not explicitly calculated, and the time difference is confined by *CFL* (Courant-Friedrich-Lewy) condition, which is defined as

$$CFL = C_i = \frac{u_i \cdot \Delta t}{l_0} \tag{11}$$

where u_i is an absolute value of the velocity and l_0 is the distance between two adjacent particles in the initial configuration. In addition, this value is different with respect to each particle in MPS. A limit is established for the maximum value of Courant number C_i as follows to keep the numerical stability.

$$\max\left(C_i\right) = \frac{\Delta t u_{\max}}{l_0} \leq C_{\max} \tag{12}$$

Because the time difference Δt and the distance between two adjacent particles l_0 are constant, the particle which Courant number C_i is equal to the maximum value C_{max} has the characteristic that the absolute value of the velocity of its particle becomes maximum value $u_{max.}$ If the time difference Δt is larger, an efficient calculation is possible. Therefore, it is desirable to use the time difference as large as possible to keep the numerical stability. Then the time difference is given as follows.

$$\Delta t = \frac{C_{\max} l_0}{u_{\max}} \tag{13}$$

The Equation (13) is calculated every time step in this study and then the size of the time difference is automatically calculated. But C_{max}=0.2 is experimentally used for an upper limitation of Courant number in anticipation of security because various factors are related to numerical stability.

3. Outline of Analyses

3.1 Purpose of analyses

In our past study, the results that the falling sediments were accelerated in the air and were sank at constant velocity were obtained by in-situ experiments (Matsumoto et al, 2011; Matsumoto et al, 2012), and the analysis results using CIP and MPS methods were agreed with the results of in-situ experiments (Isobe et al, 2012; Kawahara et al, 2012). The phenomenon that floating mud was stirred up when the sediments arrived at the seafloor was also confirmed by in-situ experiments. In this paper, even analysis proves that this phenomenon is able to be expressed, and it is a purpose to see whether sediments deposit under the floating mud after it is stirred up. Considering such a background, the parameter of a kinematic viscosity of floating mud is focused.

3.2 Analyses condition

Fig.2 shows the analysis model of the case that the sediment begins to slide from the ground above the water level assuming a coast landslide, which is case1. Fig.3 describes the case of the sediment starting to slide under the water level to simulate a submarine landslide, which is case2. The floating mud is assumed as seabed and the sediment is assumed as sandy gravel in both cases. By these assumptions, the densities of both cases are determined as shown in Table.1 but the density of the floating mud was quoted from a measured value (Miyahara et al., 2013). Also as shown in Table.1, three cases of the kinematic viscosity of the floating mud is tried to grasp the tendency from small viscosity to large one. The kinematic viscosity of the sediment is determined according to the past study (Kawahara et al, 2012). The distance between two adjacent particles and the *CFL* condition are experimentally determined in consideration of calculation time (Kawahara et al, 2012).

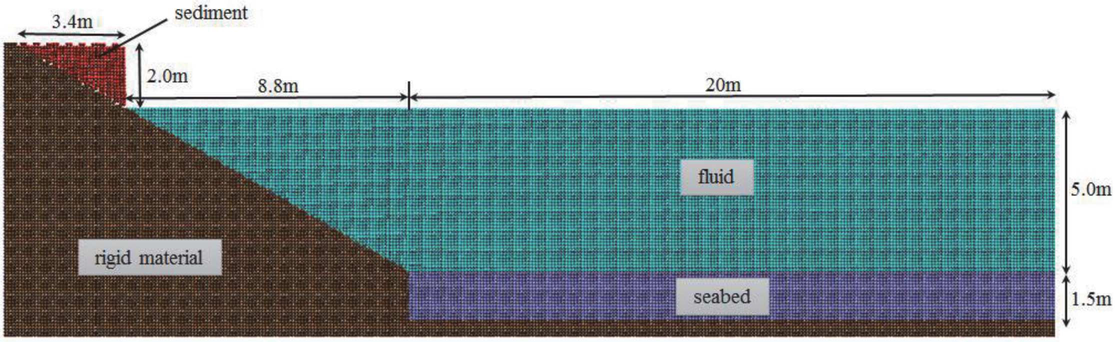

Fig. 2 Configuration of particles at 0.0 sec of case1

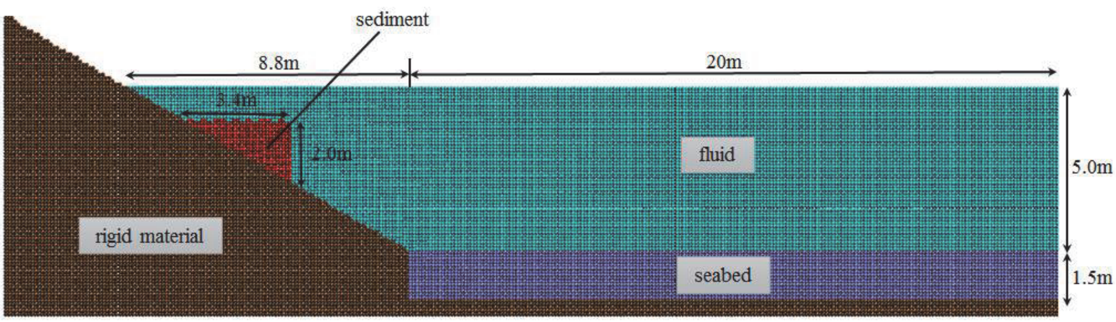

Fig. 3 Configuration of particles at 0.0 sec of case2

Table.1 Analyses parameters of both cases

parameters		unit	fluid	sediment	floating mud
density	ρ	kg/m^3	1000	2100	1300
kinematic viscosity	ν	m^2/s	1.0E-06	1.0E-03	three cases; 1.0E-02, 1.0E-03, 1.0E-4
distance between two adjacent particles	l_0	m	0.1		
gravity	g	m/s^2	9.80665		
CFL condition		-	0.2		

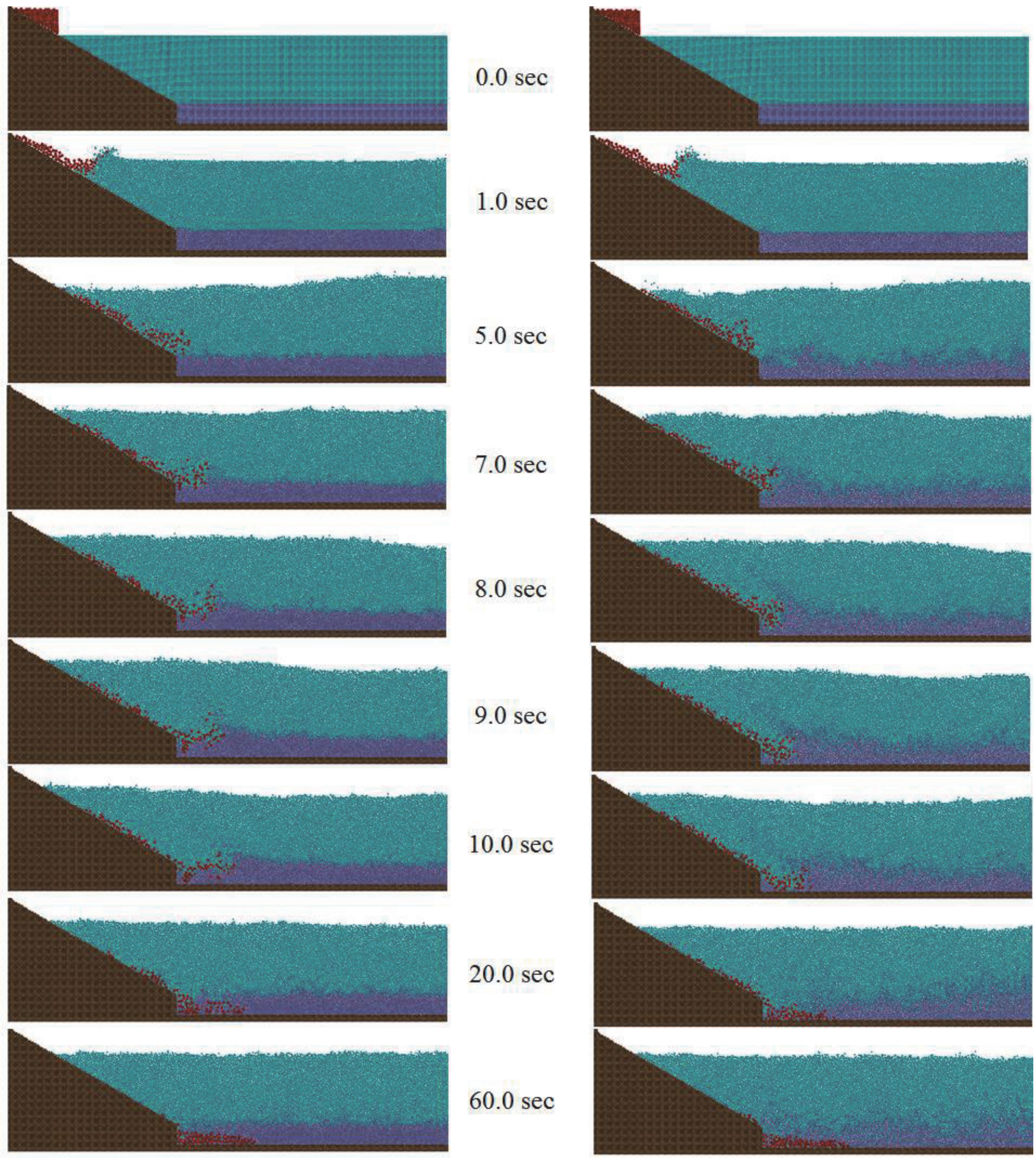

(a) kinematic viscosity of floating mud
ν=1E-02 (m^2/s)

(b) kinematic viscosity of floating mud
ν=1E-04 (m^2/s)

Fig. 4 Configuration of particles from 0.0 seconds to 60.0 seconds of case1

3.3 Results

Fig.4 shows the results of two cases within case1 to clarify the difference of kinematic viscosity of floating mud (ν), which are two order difference between ν=1E-02 (m^2/s) and ν=1E-04 (m^2/s). The sediments raise up fluid and dive into fluid at 1.0 sec in both cases. After the sediments are arrived at the seabed at 5.0 sec, the floating mud is stirred up to nearby surface of fluid by collision of the sediments from 7.0 to 10.0 sec in the case of ν=1E-04 (m^2/s). On the other hand, the state of floating mud being stirred up is not seen clearly in the case of ν=1E-02 (m^2/s).

Fig.5 shows the results of two cases within case2 as well as Fig.4. Although the collision with the fluid does not occur because of starting to slide in the fluid, the phenomenon such as case1 was similarly obtained after the sediments are arrived at the seabed. The sediments lie under the floating mud in all study cases. It is a matter of course that this is caused by density.

To focus on the configuration at 60 sec, if the kinematic viscosity is large (Fig.4,5(a)), the floating mud is not stirred up and the sediments subside into the floating mud. In contrast, if the kinematic viscosity is small (Fig.4,5(b)), the floating mud is decreased as comparison with the initial configuration because massive floating mud is stirred up. It is adequately considered that the state of the floating mud corresponding to these kinematic viscosity exists. Finally the sediments are sandwiched by the floating

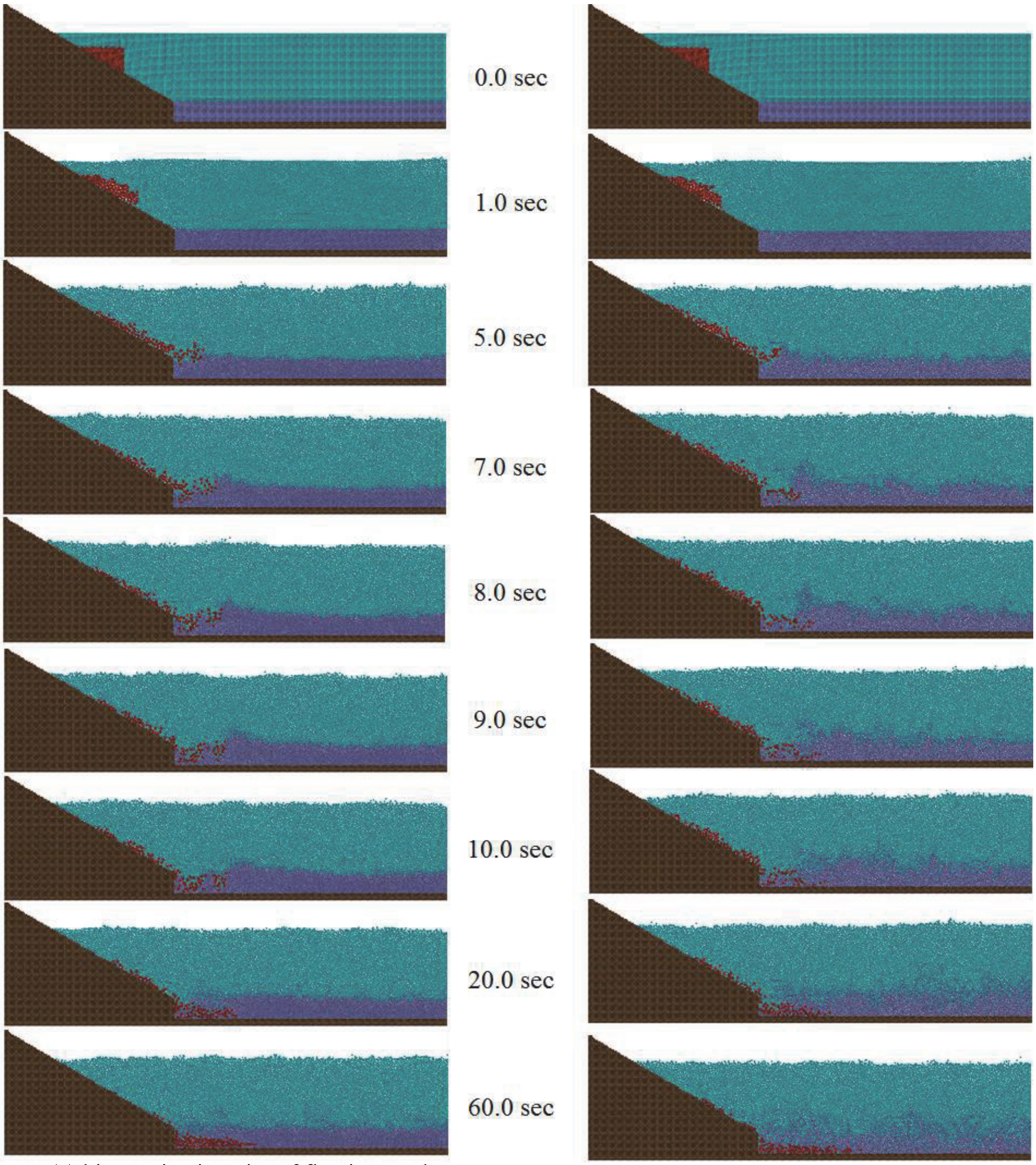

(a) kinematic viscosity of floating mud ν=1E-02 (m^2/s)

(b) kinematic viscosity of floating mud ν=1E-04 (m^2/s)

Fig. 5 Configurations of particles from 0.0 seconds to 60.0 seconds of case2 mud after accumulation of the sediments, and then the alternation of beds as shown in Photo.1 is appeared.

Although it is assumed that the density of sediments is larger than that of floating mud in this study, the study that the densities of sediments and floating mud are equal was carried out in advance. If the kinematic viscosity of the floating mud is small, it is not mixed up as shown in Fig.6. But when the value is large, like ν=1E-02, it is stirred up. This is indicated in the past study (Miyahara et al., 2013).

Therefore, stirring up the floating mud and the sediments sinking into the floating mud are caused by large difference of the density between them (floating mud < sediment) and small viscosity of the floating mud.

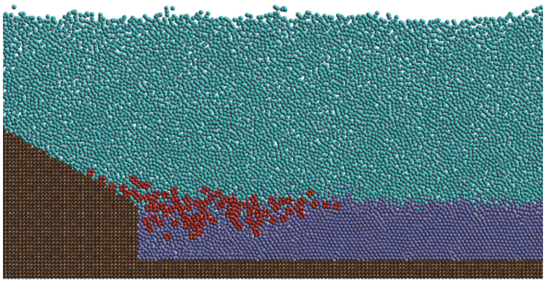

Fig. 6 Configuration of particles at 60.0 seconds when the density of the sediment is equal to the floating mud

Photo. 1 Sediments

4. Conclusions

The phenomenon that the floating mud is stirred up by collision of the sediments with the seabed and the sediments lie under the floating mud after that was able to be caught well by MPS. However, the kinematic viscosity of not only floating mud but also sediments cannot be identified because those are depended on the materials properties. The various case studies such as the depth of sea, slope angle and the amount of landslide are executed as future work.

In the occurrence of the submarine landslides, the causation with the methane hydrate is doubted (Lee, 2009). It is indicated that the landslide of the seabed which is width of 2-3km and length of 10km occurred in 2011 off the Pacific coast of Tohoku Earthquake and its relations with the tsunami are discussed (Kawamura, 2015). We think that it is possible for numerical analysis technique to be made use of for the elucidation of these phenomena.

References

Koshizuka, S. and Oka, Y. (1996): Moving-particle semi-implicit method for fragmentation of incompressible fluid, Nuclear Science and Engineering, 123, pp. 421-434.

Koshizuka, S., Nobe, A., and Oka, Y. (1998): Numerical analysis of breaking waves using the moving particle semi-implicit method, International Journal for Numerical Methods in Fluids, 26, pp. 751-769.

Matsumoto, K., Owatari, T., Ohno, H., Miyahara, T., Hachimura, T., Buma, N., and Oshima, M. (2011): Measurement and survey in water by using sonar exploration, Journal of the Japan Society of Engineering Geology, Vol. 52, No.4, pp. 128-136.

Matsumoto, K., Nagaoka, S., Ohno, H., Isobe, Y., Kawahara, H., Hachimura, T., Buma, M., Oshima, M., and Tosaka, H. (2012): Free-setting phenomenon of particles at large Reynolds numbers – free-setting experiment, Journal of the Japan Society of Engineering Geology, Vol. 53, No.2, pp. 70-79.

Isobe, Y., Kawahara, H., Matsumoto, K., Ohno, H., Tosaka, H., Nagaoka, S., Hachimura, T., Buma, M., and Oshima, M. (2012): Analysis of free-setting phenomenon of reclaimed solids at offshore disposal site by CIP method, Journal of the Japan Society of Engineering Geology, Vol. 53, No.5, pp. 218-226.

Kawahara, H., Isobe, Y., Matsumoto, K., Ohno, H., Tosaka, H., Nagaoka, S., Hachimura, T., Buma, M., and Oshima, M. (2012): Analysis of free-setting phenomenon of reclaimed solids at offshore disposal site by MPS method, Journal of the Japan Society of Engineering Geology, Vol. 53, No.5, pp. 227-234.

Miyahara, T., Nagaoka, S., Ohno, H., Hachimura, T., Kawahara, H., Isobe, Y., Hida, Y., Tomiyta, Y., and Tosaka, H. (2013): For impact phenomenon to water bottom by settling of particles in water on offshore disposal site, Journal of the Japan Society of Engineering Geology, Vol. 54, No.3, pp. 104-113.

Lee, H. J. (2009): Timing occurrence of large submarine landslides on the Atlantic Ocean margin, Marine Geology, Vol. 264, pp. 53-64.

Kawamura, K. (2015): Submarine landslides and methane hydrate in cases of Norway and Japan, Geotechnical Engineering Magazine, Vol. 63, No.2, Ser.No.685, pp. 14-17.